Use of a Multiple Hydride Donor to Achieve an n-Doped Polymer with High Solvent Resistance

Farzaneh Saeedifard,[a,b,‡] Dominique Lungwitz,[c,‡] Zi-Di Yu,[d] Sebastian Schneider,[e,f] Ahmed E Mansour,[c,g] Andreas Opitz,[c] Stephen Barlow,[a,b] Michael F Toney,[b,e,f,h] Jian Pei,[d]* Norbert Koch,[c,g]* Seth R. Marder,[a,b,i,j]*

[a] School of Chemistry and Biochemistry, Georgia Institute of Technology, Atlanta, GA 30332, USA, [b] Renewable and Sustainable Energy Institute, University of Colorado Boulder, Boulder, CO 80303, USA, [c] Institut für Physik & IRIS Adlershof, Humboldt-Universität zu, 12489 Berlin, Germany, [d] College of Chemistry and Molecular Engineering, Beijing National Laboratory for Molecular Sciences (BNLMS), Key Laboratory of Polymer Chemistry and Physics of Ministry of Education, Center of Soft Matter Science and Engineering, Peking University, Beijing 100871, China, [e] SLAC National Accelerator Laboratory, Stanford Synchrotron Radiation Light Source, Menlo Park, CA 94025, USA, [f] School of Chemistry, Stanford University, Stanford, CA 94305, USA, [g] Helmholtz-Zentrum Berlin für Materialien und Energie GmbH, 12489 Berlin, Germany, [h] Materials Science and Engineering Program, University of Colorado Boulder, Boulder, CO 80303, USA, [i] School of Chemical and Biological Engineering, University of Colorado Boulder, Boulder, CO 80303, USA, [j] School of Chemistry, University of Colorado Boulder, Boulder, CO 80303, USA.

KEYWORDS. n-doping, insolubilization, crosslinking, conductivity, hydride donor

ABSTRACT: The ability to insolubilize doped semiconducting polymer layers can help enable the fabrication of efficient multilayer solution-processed electronic and optoelectronic devices. Here, we present a promising approach to simultaneously n-dope and largely insolubilize conjugated polymer films using tetrakis[(4-(1,3-dimethyl-2,3-dihydro-1*H*-benzo[*d*]imidazol-2-yl)phenoxy)methyl]methane (tetrakis-O-DMBI-H), which consists of four 2,3-dihydro-1*H*-benzoimidazole (DMBI-H) n-dopant moieties covalently linked to one another. Doping a thiophene-fused benzodifurandione-based oligo(p-phenylenevinylene)-co-thiophene polymer (TBDOPV-T) with tetrakis-O-DMBI-H results in a highly n-doped film with bulk conductivity of 15 S cm^{-1}. Optical absorption spectra provide evidence for film retention of ca. 93% after immersion in *o*-dichlorobenzene for 5 min. The optical absorption signature of the charge carriers in the n-doped polymer decreases only slightly more than that of the neutral polymer under these conditions, indicating that the exposure to solvent also results in negligible de-doping of the film. Moreover, thermal treatment studies on a tetrakis-O-DMBI-H-doped TBDOPV-T film in contact with another undoped polymer film indicate immobilization of the molecular dopant in TBDOPV-T. This is attributed to the multiple electrostatic interactions between each dopant tetracation and up to four nearby anionic doped polymer segments.

1. INTRODUCTION

Stable and efficient doping of organic semiconductors plays an important role in a variety of (opto-)electronic devices, where it can extend the range of achievable functionality and to improve the performance of devices including organic light-emitting diodes (OLEDs), organic photovoltaic (OPV) cells, and organic field-effect transistors.[1-4] The addition of molecular oxidants (p-dopants) or reductants (n-dopants) can lead to a significant increase in the density of positive or negative charge carriers, respectively, either through simple electron-transfer reactions or more complex chemistry. This, in turn, permits one to tune the conductivity of the semiconductor, and to modulate the Fermi-level position in the semiconductor's transport gap, facilitating alignment of its charge transport levels at interfaces with those of other materials within an (opto-)electronic device stack.[5]

Although doping can help improve device performance, dopants are often prone to migration from their intended locations to other regions of the device in which their presence may not be desirable. For example, Li$^+$ ions have been found to diffuse from n-doped injection layers in OLEDs into the emissive layer, adversely affecting device performance,[6] while diffusion of much larger metal-organic dopants from a p-doped charge-extraction layer into an OPV active layer is also thought to be responsible for deterioration of device performance.[7] Furthermore, solution fabrication of multilayer devices is often challenging, in that deposition of a second layer can lead to (partial) dissolution of the first layer. Solvent-resistant polymer films have been obtained through crosslinking thermally (e.g., using benzocyclobutanes[8] or trifluorovinylethers[9]), photochemically (e.g., using acrylates[10] or cinnamates[11]), or with acid catalysis (using oxetanes[12]), allowing the fabrication of multilayer device architectures by solution-processing.[13, 14]

However, a high loading of cross-linkable units on polymer chains can in some cases interfere with the intermolecular packing and thus negatively affect the charge-carrier transport,[15, 16] and the approach will not necessarily immobilize dopant ions, unless they are also functionalized with crosslinking groups. Another approach to achieve solvent-resistant polymer films is the addition of aryl azide cross-linker molecules,[17-20] which, upon photolysis, can give highly reactive singlet nitrenes that can undergo insertion into the alkyl C–H bonds of the organic semiconductor side chains and/or dopant moieties. This can also - in principle - lead to dopant immobilization, although in a recent study molybdenum tris(dithiolene) dopants were not effectively immobilized, presumably because they contained few C–H bonds.[7] In a related approach an azide-functionalized dopant molecule has been photolyzed to covalently tether the dopant ion to a semiconductor.[21] In some cases, orthogonal solvents can be used for successive layer deposition. For example, the high-conductivity hole-injection/extraction material PEDOT:PSS (poly(3,4-ethylenedioxythiophene) polystyrene sulfonate) is usually processed from water and is insoluble in the solvents used to cast typical hole-transport materials, while the large polymeric, multiply charged counter anion PSS does not diffuse into adjacent layers. However, the water used for processing PEDOT:PSS can lead to poor long-term stability of certain devices and the approach is clearly limited to p-doping.[22]

While films resistant to solvent exposure can, at least to some extent, be created via molecular doping-induced polymer chain aggregation, the formation of aggregates has been shown in some cases to degrade the electrical properties of the film.[23] Furthermore, few n-doped materials have been reported that can be processed from solution and subsequently insolubilized,[24] especially while retaining a high conductivity.

One of the factors that makes PEDOT:PSS insoluble in low-polarity organic solvents may be a network of strong Coulombic interactions between the multiple positive charge carriers located on the PEDOT chains and the multiple negative charges on the PSS anion chain. Networks of electrostatic interactions, along with other non-covalent interactions, also play an important role in the conformations and binding characteristics of biological molecules such as proteins, and in various synthetic supramolecular self-assembling systems. We hypothesized that such “electrostatic crosslinking” could also potentially be applied to increase the solvent-exposure resistance of n-doped polymers if the dopant formed a multiply charged cation upon doping. At the same time, we considered that, if the dopant extensively reacted with the polymer at the solution-casting stage, poorly soluble material might form in an uncontrolled manner and precipitate prior to film formation. Therefore, a more desirable approach might be to use a multi-electron dopant that could be thermally activated subsequent to film formation, as shown schematically in Figure 1.

Recently, 1,3-dialkyl-2-aryl-2,3-dihydro-1*H*-benzoimidazole (DMBI-H) derivatives, especially N-DMBI-H (Figure 2), have attracted attention as n-dopants, due to their stability in air and straightforward synthesis.[25] These solution- and vacuum-processable n-dopants have been reported to undergo initial hydride transfer with at least several classes of semiconducting host materials (A), to form $DMBI^+$ cations and AH^-, which subsequently reacts further to form charge carriers, $A^{\bullet -}$,[26, 27] although other mechanisms have been suggested including loss of $H^\bullet$ atom from the dopant, with subsequent electron transfer to A from $DMBI^\bullet$,[28, 29] or from DMBI-H:A charge-transfer complexes.[30] DMBI-H derivatives have been demonstrated to dope organic semiconductor molecules, such as fullerene derivatives, and electron-transport polymers such as poly{[*N*,*N*'-bis(2-octyldodecyl)naphthalene-1,4:5,8-bis(dicarboximide)-2,6-diyl]-alt-5,5'-(2,2'-bithiophene)} [P(NDI2OD-T_2)] (Figure 2), in many cases requiring thermal treatment of the films in order to achieve efficient doping.[25-27, 31-33] Recently, conjugated polymers containing thiophene-fused benzodifurandione-based oligo(p-phenylenevinylene) (TBDOPV) monomers have exhibited film conductivity as high as 90 S cm^{-1} when doped with N-DMBI-H and thermally annealed, specifically ca. 60 S cm^{-1} in the case of TBDOPV-T, in which the TBDOPV units alternate with thiophene moieties (Figure 2), which is the polymer used in this study.[34] These conductivities, which are remarkably high for n-doped materials, are attributed to the rigid planar backbone of the polymers and excellent miscibility with the dopant molecules. Here, we describe an approach to insolubilizing n-doped films by using a new dopant, in which four DMBI-H units are connected through a saturated linking group (see Figure 2), and which is capable of forming a multiply charged cation via multiple hydride transfers.

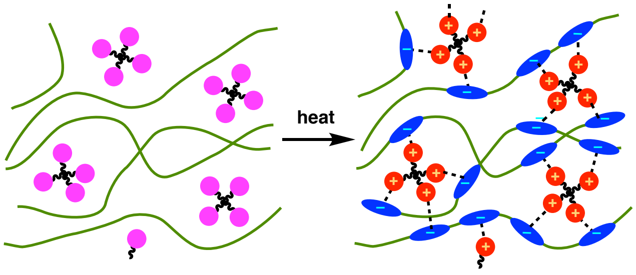

Figure 1. Schematic of “electrostatic crosslinking” between polycations (red) and negatively charged sections of polymer (blue) on thermal activation of a film containing a polymer (green) and a molecule containing multiple dopant moieties (magenta).

2. EXPERIMENTAL SECTION

2.1. General Synthesis Details. Chemicals were obtained from commercial sources and used as received unless stated otherwise. TBDOPV-T polymer[31] and MeO-DMBI-H[26] were synthesized as previously reported. P(NDI2OD-T_2) polymer, also known as N2200, was purchased from Polyera (Lot: CZH-XV-77-22). All operations involved in synthesis were performed under an atmosphere of nitrogen using standard Schlenk techniques or in a glove box. ^1H-NMR and ^{13}C-NMR spectra were recorded in $CDCl_3$ or C_6D_6, on Varian 500 or 700 MHz spectrometers. The chemical shifts (δ) are reported in parts per million (ppm). NMR spectra for tetrakis-O-DMBI-H are shown in Figure S1 and S2 in the Supporting Information.

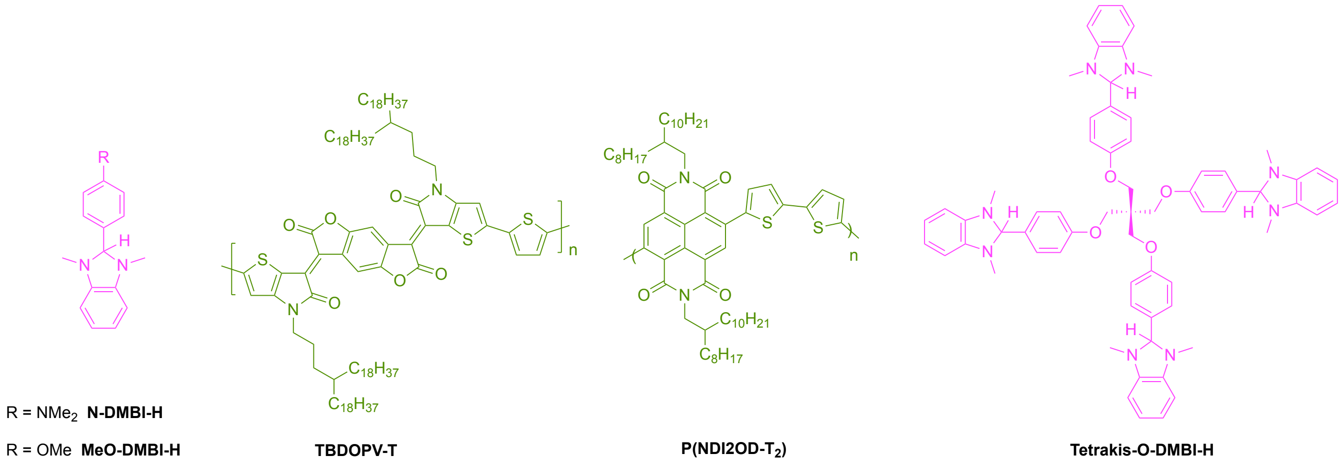

Figure 2. Chemical structures of the widely used n-dopant N-DMBI-H, the related MeO-DMBI-H, conjugated polymers P(NDI2OD-T2) and TBDOPV-T, and the tetrafunctional dopant tetrakis-O-DMBI-H discussed in this work.

2.2 Tetrakis[(4-formylphenoxy)methyl)]methane. Following a reported procedure,[32] pentaerythrityl tetrabromide (5.0 g, 12.8 mmol), 4-hydroxybenzaldehyde (7.9 g, 65 mmol), KOH (3.6 g, 65 mmol), and tetrabutylammonium iodide (40 mg, 0.11 mmol) were added to a two-neck flask. A reflux condenser was installed, and the flask evacuated and refilled with nitrogen three times. DMF (40 mL) was added, and the mixture was stirred at 120 °C for 12 h. The reaction mixture was cooled to room temperature and poured into water. The crude product was extracted with EtOAc, and washed with saturated brine, dried over sodium sulfate, and the solvents were evaporated to afford a yellow solid to which methanol (30 mL) was added. The solids were filtered and rinsed with methanol again to get yellow shiny crystals (4.0 g, 7.23 mmol, 56%). ^{1}H NMR (500 MHz, CDCl$_3$) δ 9.89 (s, 4H), 7.83 (d, J = 8.8 Hz, 8H), 7.05 (d, J = 8.8 Hz, 8H), 4.48 (s, 8H). ^{13}C{^{1}H} NMR (176 MHz, CDCl$_3$) δ 190.78, 163.27, 132.13, 130.73, 114.98, 66.58, 44.82. HRMS (ESI) calcd for $C_{33}H_{29}O_8$ (M+H$^+$), 553.1856; found 553.1850.

2.3. Tetrakis[(4-(1,3-dimethyl-2,3-dihydro-1*H*-benzo[*d*]imidazol-2-yl)phenoxy)methyl)]methane (Tetrakis-O-DMBI-H). In a glove box, tetrakis[(4-formylphenoxy)methyl)]methane (2.0 g, 3.61 mmol) was dissolved in anhydrous CH_2Cl_2 (20 mL). *N,N'*-Dimethyl-1,2-phenylenediamine (2.0 g, 14.68 mmol) was dissolved in 5.0 mL CH_2Cl_2 and added to reaction flask, which then was sealed with a septum and transferred outside the glove box. Three drops of acetic acid were added by a syringe. The mixture was stirred at RT overnight. To the mixture, methanol was added, which results in white precipitates. The solid was filtered and dissolved in CH_2Cl_2 and precipitated with methanol to obtain off-white solid (this process was repeated three times) (500 mg, 14%). ^{1}H NMR (700 MHz, C_6D_6) δ 7.42 (d, J = 8.6 Hz, 8H), 6.93 – 6.84 (m, 16H), 6.41 (dd, J = 5.4, 3.2 Hz, 8H), 4.60 (s, 4H), 4.37 (s, 8H), 2.31 (s, 24H). ^{13}C{^{1}H} NMR (176 MHz, C_6D_6) δ 160.12, 142.62, 132.58, 130.63, 119.98, 114.92, 106.28, 94.11, 67.11, 45.16, 33.05. ESI-MS = (1027.5 [M+3H]$^+$, 4.0%), 1026.5 [M+2H]$^+$, 7.9%, 1025.5 [M+H]$^+$, 0.2%), 1023.5 [M-H]$^+$. HRMS (ESI) calcd for [M-H]$^+$, 1023.5280; found 1023.5277.

2.4. Doping Experiments. Stock solutions with concentrations of 5 mg mL^{-1} for tetrakis-O-DMBI-H and TBDOPV-T were prepared under nitrogen atmosphere in an inert gas box using dried *o*-dichlorobenzene (*o*-DCB). The stock solutions were stirred overnight in order to enable complete dissolution of the materials. The reported dopant concentration, c, is given by $c = N_D / (N_D + N_P)$, where N_D is the number of dopant molecules and N_P is the number of polymer monomer units contained in the solutions. Thin films were prepared via spin-coating at 1000 rpm for 1 min, followed by 2000 rpm for 20 s. Thermal activation was performed by annealing the 9 mol%-doped thin films at 140 °C for 2.5 h on a hot plate in the glovebox, if not otherwise stated.

2.5. Film Characterization. Optical absorption spectroscopy was performed using a Lambda 950 UV-vis-NIR spectrophotometer (PerkinElmer, Inc.). Undoped and doped thin films were prepared on glass substrates with thicknesses between 5 and 20 nm. Exclusion of oxygen during the optical measurements was ensured using nitrogen-filled boxes with two quartz glass windows, in which the samples were mounted. The spectrophotometer undergoes a detector/grating and lamp change at 861 nm and 319 nm, respectively, which leads to offsets in the recorded UV-vis-NIR spectra at these positions. Therefore, the UV region (<319 nm) and NIR region (>816 nm) of the spectra were aligned to the vis region (319-861 nm) by shifting up/down with a constant offset in order to account for these artefacts.

Electrical conductivity measurements were performed inside a nitrogen-filled glovebox. The samples were prepared by spin-coating the undoped and tetrakis-O-DMBI-H-doped TBDOPV-T films on glass substrates. The sheet resistance R_S was measured by using an in-line four-point probe with 0.635 mm tip spacing, connected to a resistivity test unit (RM3000) from Jandel Engineering. Conductivity values were obtained via $\sigma = 1 / (R_S d)$, where d is the film thickness measured with a Dektak profilometer.

Ultraviolet photoelectron spectroscopy (UPS) and X-ray photoelectron spectroscopy (XPS) measurements of thin films on ITO substrates were performed in an ultrahigh vacuum chamber with a base pressure of 10^{-9} mbar. UPS measurements were performed in a custom UHV system, equipped with a monochromated helium-gas-discharge lamp (21.22 eV). For XPS measurements, non-monochromated Al Kα (1486.7 eV) radiation was used for excitation. The spectra were collected in normal emission with a SPECS Phoibos 100 hemispherical electron energy analyzer. The pass energy was 5 eV or 20 eV for UPS and XPS measurements, respectively. The secondary electron cutoff (SECO) spectra were measured with a bias of −10 V, which was applied to the sample in order to clear the analyzer work function.

Film surface topography (Figure S3, Supporting Information) was characterized with a Bruker Dimension Icon scanning force microscope, operated in Peak Force Tapping TM mode using ScanAsyst-Air cantilevers. Grazing incidence wide angle X-ray scattering (GIWAXS) measurements (Figure S4, Supporting Information) were performed at the Stanford Synchrotron Radiation Lightsource (SSRL) beamline 11–3 with an X-ray wavelength of 0.9752 Å and sample-to-detector distance of 321 mm at an incident angle of 0.14°. Measurements were carried out using a He-filled sample chamber to reduce air scattering background. The spectra were collected with a 2D CCD X-ray detector (MX225, Rayonix, L.L.C) with a pixel size of 73.2 µm (3072 × 3072 pixels)

3. RESULTS AND DISCUSSION

3.1. Dopant Design, Synthesis, and Use. As discussed in the introduction, we chose a molecule using multiple DMBI-H dopant moieties since, at least with many semiconductors, doping with these moieties requires thermal activation, enabling doping and insolubilization to be achieved subsequent to film formation. We chose a pentaerythritol-based core to connect our multiple dopant moieties due to: its ready availability; its relatively small size, which will not excessively dilute the active components of the doped film and may help minimize structural disruption; and its non-rigidity, which was anticipated to facilitate solubility of dopant precursors and the dopant itself, as well as allowing the conformation of the molecule to adapt to different host environments. Moreover, $C(CH_2Br)_4$ can be converted to tetrakis[(4-formylphenoxy)methyl)]methane through a straightforward literature procedure,[32] which can potentially serve as a precursor to tetrakis-O-DMBI-H (Figure 2), in which there are π-electron-donating alkoxy substituents on the 2-aryl groups of the DMBI-H moieties. These π-donors accelerate the hydride-transfer step through stabilization of the highly polarized transition state that ultimately results in formation of the corresponding benzimidazolium cation,[26] and the alkoxy groups in tetrakis-O-DMBI-H are anticipated to lead to a reactivity similar to, albeit somewhat lower than, that of N-DMBI-H, which is appropriate for thermally activated doping of polymers including TBDOPV-T and P(NDI2OD-T_2).[25-27, 31-34]

Tetrakis[(4-formylphenoxy)methyl)]methane has reasonable solubility in CH_2Cl_2, which is commonly used for the synthesis of DMBI-H derivatives. Accordingly, this aldehyde was converted to tetrakis-O-DMBI-H through condensation of tetrakis[(4-formylphenoxy)methyl)]methane and *N*,*N*′-dimethyl-1,2-phenylenediamine in the presence of a catalytic amount of acetic acid in CH_2Cl_2, in analogy to reported syntheses of monomeric DMBI-H derivatives.[33]

Films of TBDOPV-T doped with various concentrations of tetrakis-O-DMBI-H were fabricated by spin-coating from *o*-dichlorobenzene solution (*o*-DCB) and thermally activating at 140 °C for 2.5 h. As discussed in section 3.3, appreciable doping is not observed without the thermal annealing step.

3.2. UPS Studies of Doping. UPS was used to investigate changes in the electronic structure of TBDOPV-T on reaction with tetrakis-O-DMBI-H (Figure 3). The pristine TBDOPV-T film on ITO exhibited a work function of 4.6 eV and an ionization energy of 5.0 eV; i.e., the Fermi level (E_F) was ca. 0.4 eV above the valence band onset. After the thermal activation step, a film of TBDOPV-T doped with 9 mol% tetrakis-O-DMBI-H (i.e., 36 mol% hydride, the concentration examined that afforded the highest electron conductivity, see section 3.5) exhibited a reduced work function of 4.0 eV, and an additional density of states extending up to E_F. Negative charge carriers in the form of polarons or bipolarons on conjugated polymers result in two gap states, i.e., an occupied state just below the conduction band and another state just above the valence band of the neutral polymer.[34,35] In the valence spectra of Figure 3b we cannot resolve two gap states, but rather two seemingly merged features (a peak at ca. 5.5 eV and the shoulder at ca. 4.5 eV) seem to fill the former transport gap of the polymer. Given that TBDOPV-T is a narrow-gap semiconductor (optical gap of 0.9 eV), it is conceivable that the two doping-induced gap states appear merged, particularly in the presence of structural and electrostatic disorder. The upper onset of the gap state(s) is just below E_F, so that the 9 mol% tetrakis-O-DMBI-H-doped TBDOPV-T film exhibits an ionization energy of only 4.0 eV. All these observations are consistent with n-doping.

We assume doping of TBDOPV-T using tetrakis-O-DMBI-H takes place via an initial hydride transfer, with subsequent reactions leading to polaron and/or bipolaron charge carriers, in analogy to what has been seen for the reaction of N-DMBI-H and 2CN-BDOPV, a small molecule similar to the electron-poor monomer unit of TBDOPV-T.[27] Certainly ion-pair formation via a simple one-electron transfer can be excluded; UPS affords an ionization energy of 5.4 eV for tetrakis-O-DMBI-H (higher than that of TBDOPV-T) and the electron affinity of TBDOPV-T can be estimated to be around 3.9 eV (see Figure S5 for further details), indicating that such an electron-transfer reaction would be endergonic by well over 1 eV and thus the rates of electron transfer would be slow at the temperatures used to process the film and the equilibrium constant for ion-pair formation even smaller than that for thermal formation of carriers in the undoped polymer.

3.3. Optical Studies of Doping and Insolubilization. Optical absorption spectroscopy was performed to provide further evidence for doping of the polymer with tetrakis-O-DMBI-H (see Figure 4a). The spectrum of a 9 mol% tetrakis-O-DMBI-H-doped TBDOPV-T film thermally annealed at 140 °C for 2.5 h shows the emergence of a new absorption feature at ca. 0.7 eV attributed to the charge carriers introduced on doping. Simultaneously, the features of the neutral polymer at about 1.1 eV and 2.6 eV are bleached, as expected as the proportion of neutral TBDOPV-T segments is reduced. These spectral changes are similar to those previously found on n-doping the same polymer with the monomeric hydride-donor dopant, N-DMBI-H, and with $(RuCp^*mes)_2$ ($Cp^* = C_5Me_5$; mes = mesitylene).[31] In particular, the changes in the spectrum are similar to those observed with N-DMBI-H at similar reactive hydride concentrations suggesting a similarly high charge-generation efficiency (XPS suggests most N-DMBI-H units in annealed TBODPV-T films are converted to N-DMBI$^+$). We note that thermal activation of the dopant:polymer film is necessary for the observation of doping; the absorption feature at 0.7 eV is not observed in the UV-vis.-NIR spectrum of the tetrakis-O-DMBI-H:TBDOPV-T film prior to thermal activation (Figure S6 in the Supporting Information).

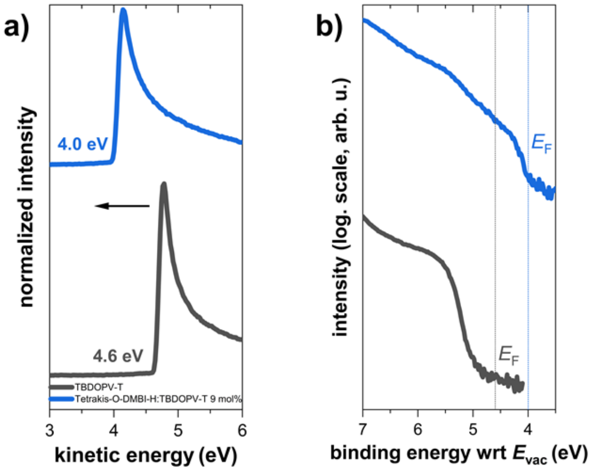

Figure 3. UPS a) secondary electron cutoff (SECO) and b) valence spectra of pristine and tetrakis-O-DMBI-H-doped TBDOPV-T films. The numbers next to the SECO spectra are the corresponding work-function values. Valence spectra are plotted on a logarithmic intensity scale to emphasize the polymer's valence band features; on a linear intensity scale these are barely visible due to the long polymer sidechains that attenuate the photoelectrons from the conjugated backbone.

The 140 °C-annealed tetrakis-O-DMBI-H-doped films are visually unaffected by brief immersion in solvents including *ortho*-dichlorobenzene (*o*-DCB), THF, and CH_2Cl_2. The *o*-DCB resistance was quantified by immersing the doped film in that solvent for 5 min. The absorbance of the neutral feature at 1.1 eV decreased only slightly, to 93% of its initial value. The absorbance of the feature at 0.7 eV assigned to the charge carriers shows a slightly larger decrease, but the ratio of absorbance at 0.7 eV to that at 1.1 eV decreases by only ca. 3%. On the other hand, neither the pristine polymer nor the dopant:polymer film without thermal activation shows any resistance to *o*-DCB immersion under the same conditions (Figure S6a, Supporting Information, consistent with our original hypothesis that the resistance to solvent is the Coulombic attraction between multi-charged cations and the charged polymer segments after doping, rather than a consequence of changes in morphology or microstructure induced by the presence of dopant molecules (see following section). Annealing at lower temperatures leads to more limited solvent resistance (Figure S6b).

As a further control experiment, we also examined the effect of *o*-DCB upon annealed MeO-DMBI-H-doped TBDOPV-T. MeO-DMBI-H was chosen as a monomeric model for tetrakis-O-DMBI-H capable of transferring only one hydride to form a monocation, but with similar electronic structure, and was used at a comparable hydride concentration. A very large decrease in the absorbance of both neutral and charge-carrier features is observed after immersing the doped film in *o*-DCB (Figure S7 in the Supporting Information). This observation further supports the idea that the high *o*-DCB resistance of tetrakis-O-DMBI-H-doped TBDOPV-T films can be ascribed to the strong electrostatic interactions between multiply charged cations and the neighboring negatively charged polymer chains.

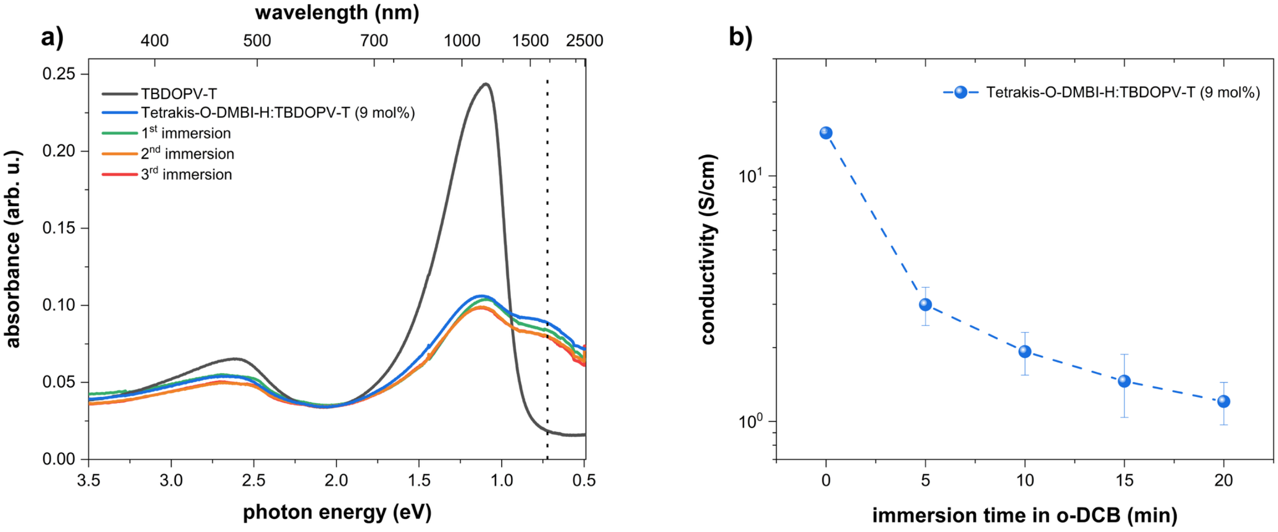

Figure 4. a) Optical absorption spectra of undoped TBDOPV-T and annealed tetrakis-O-DMBI-H-doped TBDOPV-T films before and after immersing in *o*-DCB for 5 min (see also Figures S6 and S7 for control experiments). The optical transition assigned to the TBDOPV-T charge carrier at 0.7 eV is marked with a dotted line. b) Electrical conductivity of annealed tetrakis-O-DMBI-H-doped TBDOPV-T films before and after immersing in *o*-DCB.

3.4. Morphology and Microstructure. Changes in the morphology and polymer ordering were observed upon doping with tetrakis-O-DMBI-H and annealing, as revealed by scanning force microscopy (SFM) and grazing-incidence wide-angle X-ray scattering (GIWAXS) characterization, respectively (Figures S3 and S4 in the Supporting Information). GIWAXS shows that the doping of TBDOPV-T with tetrakis-O-DMBI-H led to broader diffraction peaks, indicating an increase in structural disorder. SFM also indicates that the doped films are somewhat smoother, consistent with a reduction in crystallinity. This behavior is found for many doped systems,[39] although previous studies of TBDOPV doped with the smaller monomeric N-DMBI-H led to slightly *increased* order.[31] In the present work, slight increases of both (100) and (010) plane-spacing using tetrakis-O-DMBI-H was observed, where (100) and (010) denote the planes defined by the lamellae formed by the polymers and by the π–π stacking, respectively. For a tetrakis-O-DMBI-H fraction of 9 mol%, the (100) spacing increased from 34.5 Å to 36.0 Å, similar to what was seen on doping with N-DMBI-H.[31] The π–π stacking distance increased from 3.39 Å to 3.45 Å with 9 mol% tetrakis-O-DMBI-H, whereas the use of N-DMBI-H had little effect on the π–π stacking spacing.[31] The increased structural disorder seen with increased dopant concentration is unlikely to explain the solvent-exposure resistance of the doped films since more crystalline systems are typically less soluble than disordered systems.

3.5. Electrical Conductivity. The bulk electrical conductivity of annealed TBDOPV-T films with 5 and 9 mol% tetrakis-O-DMBI-H-dopant (i.e., 20 and 36 mol% hydride, close to 28-33 mol% range of N-DMBI-H concentrations leading to maximum conductivity in TBDOPV-T[31]) was measured with four-point probe as a function of immersion time (Figure 4b). Since the conductance of the pristine TBDOPV-T film was too low to be determined with our setup, a value of 1×10^{-7} S cm^{-1} (the detection limit of the measurement system used) can be taken as upper limit for the conductivity of the undoped material. The films with 5 and 9 mol% dopant prior to solvent immersion exhibited conductivity values of ca. 1 and 15 S cm^{-1} respectively. This enhancement of conductivity by 7+ and 8+ orders of magnitude at 5 and 9 mol% dopant, respectively, is clearly consistent with the effective doping suggested by UPS and UV-vis-NIR spectroscopy. These conductivity values are still considerably lower than obtained for the same polymer n-doped by N-DMBI-H, which forms a more-or-less planar cation, but are similar to those obtained using $(\mathrm{RuCp^{*}mes})_2$, an organometallic dopant that forms a three-dimensional cation.[31] The reduction in polymer order (Figure S4) by the somewhat bulky three-dimensional tetrafunctional dopant used here may play a role in obtaining a lower conductivity than using the chemically similar N-DMBI-H. To test the stability of the electrical properties of the doped film to solvent treatment, it was immersed in *o*-DCB for 5 min, resulting in a drop of conductivity to 3 S cm^{-1}. After further immersion steps, the conductivity changed moderately. These data provide further evidence for the high stability of the annealed tetrakis-O-DMBI-H-doped semiconductor polymer film to solvent. The apparent discrepancy between the minor change in absorption spectrum, suggesting a minor change in carrier concentration, and the five-fold decrease in conductivity after immersion presumably largely reflects a decrease in charge-carrier mobility. Since the film retention is about 93%, a small fraction of the doped polymer film is obviously removed by the solvent. However, it is also reasonable to assume that some solvent molecules are able to diffuse into the film when immersed in *o*-DCB. Although the films were dried under a stream of nitrogen, we speculate that residual solvent molecules could affect the film microstructure leading to the observed decrease in conductivity.

3.6. Dopant Diffusion. The multiple electrostatic interaction between dopant ions and charged polymer segments that we consider likely responsible for the solvent-exposure resistance of tetrakis-O-DMBI-H-doped TBDOPV-T films, along with the large size of the dopant, might also be expected to suppress diffusion of the dopant. Before examining the possibility of dopant molecule and/or ion diffusion into an undoped polymer layer, we established that a film of tetrakis-O-DMBI-H-doped TBDOPV-T was stable to thermal annealing (140 °C for 5 h in an inert atmosphere, see Figure S9a). We then examined the ability of tetrakis-O-DMBI-H and/or tetrakis-O-DMBI-H-derived cations to diffuse from a thermally activated tetrakis-O-DMBI-H-doped TBDOPV-T film into an adjacent undoped film.

We chose polymer P(NDI2OD-T_2) (Figure 2) as a suitable undoped material since it meets several key requirements for investigating dopant diffusion using absorption spectroscopy. Firstly, its reduction potential is very similar to that of TBDOPV-T (both are ca. –1.0 V vs. ferrocene),[31, 40] and so no energetic penalty is expected for dopant ion and charge-carrier migration from TBDOPV-T into P(NDI2OD-T_2). Secondly, the spectra of neutral and reduced P(NDI2OD-T_2) are distinct from those of neutral and reduced TBDOPV-T.[41] Importantly, despite differences in backbone rigidity, charge delocalization, and side-chain spacing, all of which could potentially affect dopant diffusion, a control experiment showed P(NDI2OD-T_2) can be doped sequentially using tetrakis-O-DMBI-H after thermal annealing (Figure S9b). This indicates that at least neutral tetrakis-O-DMBI-H can diffuse into the film and that any such diffusing unreacted dopant would dope this polymer. Accordingly, a P(NDI2OD-T_2) film was deposited on a tetrakis-O-DMBI-H doped TBDOPV-T film that had been thermally activated; this bilayer structure was then heated at 140 °C for 3 h in an inert atmosphere. Migration of dopant ions and associated charge carriers (or migration and activation of any unreacted dopants) would be expected to result in the appearance of the absorption features characteristic of P(NDI2OD-T_2) charge carriers (ca. 2.5 and 1.5 eV[41]), increased neutral TBDOPV-T absorbance (ca. 1.2 eV), and a decrease in absorbance attributable to neutral P(NDI2OD-T_2) (ca. 3.1 and 1.8 eV and to TBDOPV-T charge carriers (ca. 0.7 eV). As can be seen from Figure 5, changes are slight (no changes at 0.7, 1.2, and 3.1 eV, slight increases at 2.5 and 1.2 eV, slight decrease at 1.8 eV eV). Thus, under these conditions, there is evidently minimal diffusion of tetrakis-O-DMBI-H-derived ions into P(NDI2OD-T_2).

4. CONCLUSION

In conclusion, a molecule in which four DMBI-H units are linked together via a saturated carbon center – tetrakis-O-DMBI-H – n-dopes the electron-transporting polymers P(NDI2OD-T_2) and TBDOPV-T after thermal annealing. An annealed tetrakis-O-DMBI-H-doped-TBDOPV-T film exhibited a conductivity of 15 S cm^{-1}, coupled with good resistance to *o*-DCB, which we ascribe to strong electrostatic interactions between multiply charged cations and the neighboring negatively charged polymer chains. No evidence was found for the diffusion of dopant molecules and ions from a tetrakis-O-DMBI-H-doped-TBDOPV-T into a P(NDI2OD-T$_2$) film, an observation that may be due both to the same strong dopant ion:polymer interactions responsible for increased solvent-exposure resistance and to the large size of the dopant ions. Accordingly, this work suggests a possible means of fabricating multilayer structures from solution and restricting to intentionally doped regions of devices. More dopant:polymer combinations will be investigated in the future to establish the generality and limitations of the approach.

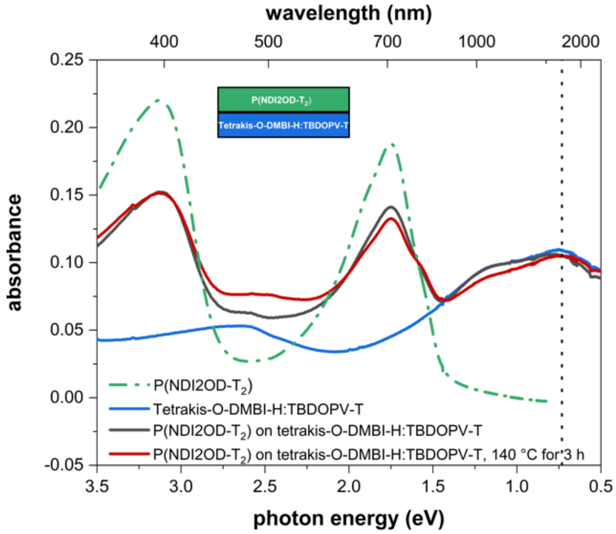

Figure 5. Optical absorption spectra of films of P(NDI2OD-T$_2$), tetrakis-O-DMBI-H-doped TBDOPV-T, and P(NDI2OD-T$_2$) deposited onto tetrakis-O-DMBI-H-doped TBDOPV-T films before and after heating at 140 °C. The vertical dashed line indicates the feature attributable to TBDOPV-T charge carriers.

ASSOCIATED CONTENT

Supporting Information

The Supporting Information is available free of charge on the ACS Publications website.

NMR spectra for tetrakis-O-DMBI-H, additional UPS data, SFM and GIWAXS data, additional optical spectra of films under various conditions (PDF)

AUTHOR INFORMATION

Corresponding Author

* Email: jianpei@pku.edu.cn (J.P.)
* Email: norbert.koch@physik.hu-berlin.de (N.K.)
* Email: seth.marder@colorado.edu (S.R.M.)

Author Contributions

‡These authors contributed equally.

Notes

The authors declare no competing financial interest.

ACKNOWLEDGMENT

This work was supported by the Deutsche Forschungsgemeinschaft (DFG) – project number 239543752, the National Science Foundation (through DMR-807797/2216857 and through the DMREF program, DMR-1729737), and the US Air Force of Scientific Research (FA9550-18-1-0499). The authors thank Paul Zybarth for technical support throughout conductivity measurements.

REFERENCES

(1) Murawski, C.; Fuchs, C.; Hofmann, S.; Leo, K.; Gather, M. C., Alternative p-Doped Hole Transport Material for Low Operating Voltage and High Efficiency Organic Light-Emitting Diodes. *Appl. Phys.* **2014,** *105*, 113303.

(2) Bin, Z. Y.; Liu, Z. Y.; Qiu, Y.; Duan, L., Efficient n-Dopants and Their Roles in Organic Electronics. *Adv. Opt. Mater.* **2018,** *6*, 1800536.

(3) Selzer, F.; Falkenberg, C.; Hamburger, M.; Baumgarten, M.; Müllen, K.; Leo, K.; Riede, M., Improved Organic p-i-n Type Solar Cells with n-Doped Fluorinated Hexaazatrinaphthylene Derivatives HATNA-F$_6$ and HATNA-F$_{12}$ as Transparent Electron Transport Material. *J. Appl. Phys.* **2014,** *115*, 054515.

(4) Lüssem, B.; Keum, C.-M.; Kasemann, D.; Naab, B.; Bao, Z.; Leo, K., Doped Organic Transistors. *Chem. Rev.* **2016,** *116*, 13714-13751.

(5) Walzer, K.; Maennig, B.; Pfeiffer, M.; Leo, K., Highly Efficient Organic Devices Based on Electrically Doped Transport Layers. *Chem. Rev.* **2007,** *107*, 1233-1271.

(6) D'Andrade, B. W.; Forrest, S. R.; Chwang, A. B., Operational Stability of Electrophosphorescent Devices Containing p and n Doped Transport Layers. *Appl. Phys.* **2003,** *83*, 3858-3860.

(7) Dahlström, S.; Wilken, S.; Zhang, Y.; Ahläng, C.; Barlow, S.; Nyman, M.; Marder, S. R.; Österbacka, R., Cross-Linking of Doped Organic Semiconductor Interlayers for Organic Solar Cells: Potential and Challenges. *ACS Appl. Energy Mater.* **2021,** *4*, 14458-14466.

(8) Ma, B.; Lauterwasser, F.; Deng, L.; Zonte, C. S.; Kim, B. J.; Fréchet, J. M. J.; Borek, C.; Thompson, M. E., New Thermally Cross-Linkable Polymer and its Application as a Hole-Transporting Layer for Solution Processed Multilayer Organic Light Emitting Diodes. *Chem. Mater.* **2007,** *19*, 4827-4832.

(9) Niu, Y.-H.; Liu, M. S.; Ka, J.-W.; Jen, A. K.-Y., Thermally Crosslinked Hole-Transporting Layers for Cascade Hole-Injection and Effective Electron-Blocking/Exciton-Confinement in Phosphorescent Polymer Light-Emitting Diodes. *Appl. Phys.* **2006,** *88*, 093505.

(10) Bacher, A.; Erdelen, C. H.; Paulus, W.; Ringsdorf, H.; Schmidt, H.-W.; Schuhmacher, P., Photo-Cross-Linked Triphenylenes as Novel Insoluble Hole Transport Materials in Organic LEDs. *Macromolecules* **1999,** *32*, 4551-4557.

(11) Li, X. C.; Yong, T. M.; Gruner, J.; Holmes, A. B.; Moratti, S. C.; Cacialli, F.; Friend, R. H., A Blue Light Emitting Copolymer with Charge Transporting and Photo-Crosslinkable Functional Units. *Synth. Met.* **1997,** *84*, 437-438.

(12) Bayerl, M. S.; Braig, T.; Nuyken, O.; Muller, D. C.; Gross, M.; Meerholz, K., Crosslinkable Hole-Transport Materials for Preparation of Multilayer Organic Light Emitting Devices by Spin-Coating. *Macromol. Rapid Commun.* **1999,** *20*, 224-228.

(13) Zuniga, C. A.; Barlow, S.; Marder, S. R., Approaches to Solution-Processed Multilayer Organic Light-Emitting Diodes Based on Cross-Linking. *Chem. Mater.* **2011,** *23*, 658-681.

(14) Kahle, F. J.; Saller, C.; Kohler, A.; Strohriegl, P., Crosslinked Semiconductor Polymers for Photovoltaic Applications. *Adv. Energy Mater.* **2017,** *7*, 1700306.

(15) Bellmann, E.; Shaheen, S. E.; Thayumanavan, S.; Barlow, S.; Grubbs, R. H.; Marder, S. R.; Kippelen, B.; Peyghambarian, N., New Triarylamine-Containing Polymers as Hole Transport Materials in Organic Light-Emitting Diodes: Effect of Polymer Structure and Cross-Linking on Device Characteristics. *Chem. Mater.* **1998,** *10*, 1668-1676.

(16) Zhang, Y.-D.; Hreha, R. D.; Jabbour, G. E.; Kippelen, B.; Peyghambarian, N.; Marder, S. R., Photo-Crosslinkable Polymers as Hole-Transport Materials for Organic Light-Emitting Diodes. *J. Mater. Chem.* **2002,** *12*, 1703-1708.

(17) Park, J.; Lee, C.; Jung, J.; Kang, H.; Kim, K. H.; Ma, B. W.; Kim, B. J., Facile Photo-Crosslinking of Azide-Containing Hole-Transporting Polymers for Highly Efficient, Solution-Processed, Multilayer Organic Light Emitting Devices. *Adv. Funct. Mater.* **2014,** *24*, 7588-7596.

(18) Teo, D. W. Y.; Jamal, Z.; Phua, H.-Y.; Tang, C. G.; Png, R.-Q.; Chua, L.-L., Nearly 100% Photocrosslinking Efficiency in Ultrahigh Work Function Hole-Doped Conjugated Polymers using Bis(fluorophenyl azide) Additives. *ACS Appl. Mater. Interfaces.* **2019,** *11*, 48103-48112.

(19) Kim, M. J.; Lee, M.; Min, H.; Kim, S.; Yang, J.; Kweon, H.; Lee, W.; Kim, D. H.; Choi, J.-H.; Ryu, D. Y.; Kang, M. S.; Kim, B.; Cho, J. H., Universal Three-Dimensional Crosslinker for All-Photopatterned Electronics. *Nat. Commun.* **2020,** *11*, 1520.

(20) Png, R.-Q.; Chia, P.-J.; Tang, J.-C.; Liu, B.; Sivaramakrishnan, S.; Zhou, M.; Khong, S.-H.; Chan, H. S. O.; Burroughes, J. H.; Chua, L.-L.; Friend, R. H.; Ho, P. K. H., High-Performance Polymer Semiconducting Heterostructure Devices by Nitrene-Mediated Photocrosslinking of Alkyl Side Chains. *Nat. Mater.* **2010,** *9*, 152-158.

(21) Reiser, P.; Benneckendorf, F. S.; Barf, M. M.; Muller, L.; Bauerle, R.; Hillebrandt, S.; Beck, S.; Lovrincic, R.; Mankel, E.; Freudenberg, J.; Jansch, D.; Kowalsky, W.; Pucci, A.; Jaegermann, W.; Bunz, U. H. F.; Mullen, K., n-Type Doping of Organic Semiconductors: Immobilization via Covalent Anchoring. *Chem. Mater.* **2019,** *31*, 4213-4221.

(22) Cameron, J.; Skabara, P. J., The Damaging Effects of the Acidity in PEDOT:PSS on Semiconductor Device Performance and Solutions Based on Non-Acidic Alternatives. *Mater. Horiz.* **2020,** *7*, 1759-1772.

(23) Jacobs, I. E.; Aasen, E. W.; Oliveira, J. L.; Fonseca, T. N.; Roehling, J. D.; Li, J.; Zhang, G.; Augustine, M. P.; Mascal, M.; Moulé, A. J., Comparison of Solution-Mixed and Sequentially Processed P3HT:F$_4$TCNQ Films: Effect of Doping-Induced Aggregation on Film Morphology. *J. Mater. Chem. C* **2016,** *4*, 3454-3466.

(24) Tremblay, M.-H.; Schutt, K.; Pulvirenti, F.; Schultz, T.; Wegner, B.; Jia, X.; Zhang, Y.; Longhi, E.; Dasari, R. R.; Fuentes-Hernandez, C.; Kippelen, B.; Koch, N.; Snaith, H. J.; Barlow, S.; Marder, S. R., Benzocyclobutene Polymer as an Additive for a Benzocyclobutene-Fullerene: Application in Stable p–i–n Perovskite Solar Cells. *J. Mater. Chem.* **2021,** *9*, 9347-9353.

(25) Wei, P.; Oh, J. H.; Dong, G. F.; Bao, Z. N., Use of a 1*H*-Benzoimidazole Derivative as an n-Type Dopant and to Enable Air-Stable Solution-Processed n-Channel Organic Thin-Film Transistors. *J. Am. Chem. Soc.* **2010,** *132*, 8852-8853.

(26) Naab, B. D.; Guo, S.; Olthof, S.; Evans, E. G. B.; Wei, P.; Millhauser, G. L.; Kahn, A.; Barlow, S.; Marder, S. R.; Bao, Z. A., Mechanistic Study on the Solution-Phase n-Doping of 1,3-Dimethyl-2-aryl-2,3-dihydro-1*H*-benzoimidazole Derivatives. *J. Am. Chem. Soc.* **2013,** *135*, 15018-15025.

(27) Jhulki, S.; Un, H. I.; Ding, Y. F.; Risko, C.; Mohapatra, S. K.; Pei, J.; Barlow, S.; Marder, S. R., Reactivity of an Air-Stable Dihydrobenzoimidazole n-Dopant with Organic Semiconductor Molecules. *Chem* **2021,** *7*, 1050-1065.

(28) Kwon, G.; Kim, K.; Choi, B. D.; Roh, J.; Lee, C.; Noh, Y. Y.; Seo, S.; Kim, M. G.; Kim, C., Multifunctional Organic-Semiconductor Interfacial Layers for Solution-Processed Oxide-Semiconductor Thin-Film Transistor. *Adv. Mater.* **2017,** *29*.

(29) Rossbauer, S.; Muller, C.; Anthopoulos, T. D., Comparative Study of the n-Type Doping Efficiency in Solution-Processed Fullerenes and Fullerene Derivatives. *Adv. Funct. Mater.* **2014,** *24*, 7116-7124.

(30) Schlitz, R. A.; Brunetti, F. G.; Glaudell, A. M.; Miller, P. L.; Brady, M. A.; Takacs, C. J.; Hawker, C. J.; Chabinyc, M. L., Solubility-Limited Extrinsic n-Type Doping of a High Electron Mobility Polymer for Thermoelectric Applications. *Adv. Mater.* **2014,** *26*, 2825-2830.

(31) Lu, Y.; Yu, Z. D.; Un, H. I.; Yao, Z. F.; You, H. Y.; Jin, W. L.; Li, L.; Wang, Z. Y.; Dong, B. W.; Barlow, S.; Longhi, E.; Di, C. A.; Zhu, D. B.; Wang, J. Y.; Silva, C.; Marder, S. R.; Pei, J., Persistent conjugated backbone and disordered Lamellar Packing Impart Polymers with Efficient n-Doping and High Conductivities. *Adv. Mater.* **2021,** *33*, 2005946.

(32) Kungurtsez, V.; Laakkonen, J.; Gimenez Molina, A.; Virta, P., Solution-Phase Synthesis of Short Oligo-2'-deoxyribonucleotides by Using Clustered Nucleosides as a Soluble Support. *Eur. J. Org. Chem.* **2013,** *2013*, 6687-6693.

(33) Zhu, X.-Q.; Zhang, M.-T.; Yu, A.; Wang, C.-H.; Cheng, J.-P., Hydride, Hydrogen Atom, Proton, and Electron Transfer Driving Forces of Various Five-Membered Heterocyclic Organic Hydrides and Their Reaction Intermediates in Acetonitrile. *J. Am. Chem. Soc.* **2008,** *130*, 2501-2516.

(34) Heimel, G., The Optical Signature of Charges in Conjugated Polymers. *ACS Cent. Sci.* **2016,** *2*, 309-315.

(35) Png, R.-Q.; Ang, M. C. Y.; Teo, M.-H.; Choo, K.-K.; Tang, C. G.; Belaineh, D.; Chua, L.-L.; Ho, P. K. H., Madelung and Hubbard Interactions in Polaron Band Model of Doped Organic Semiconductors. *Nat. Commun.* **2016,** *7*, 11948.

(36) Bin, Z.; Li, J.; Wang, L.; Duan, L., Efficient n-Type Dopants with Extremely Low Doping Ratios for High Peformance Inverted Perovskite Solar Cells, *Energy Environ. Sci*. **2016**, *9*, 3424-3428.

(37) Riera-Galindo, S.; Biroli, A. O.; Forni, A.; Puttisong, Y.; Tessore, F.; Pizzotti, M.; Pavlopoulou, E.; Solano, E.; Wang, S.; Wang, G.; Chen, W. M.; Kemerink, M.; Berggren, M.; di Carlo, G.; Fabiano, S., Impact of Singlyb Occupied Molecular Orbital Energy on the n-Doping Efficiency of Benzimidazole Derivatives, *ACS Appl. Mater. Interfaces*, **2019**, *11*, 37981-37990.

(38) Zeng, Y.; Zheng, W.; Guo, Y.; Han, G.; Yi, Y., Doping Mechanisms of N-DMBI-H for Organic Thermoelectrics: Hydrogen Removal vs. Hydride Transfer, *J. Mater. Chem. A*, **2020**, 8, 8323-8328.

(39) Duong, D. T.; Wang, C. C.; Antono, E.; Toney, M. F.; Salleo, A., The Chemical and Structural Origin of Efficient p-Type Doping in P3HT. *Org. Electron.* **2013,** *14*, 1330-1336.

(40) Guo, X.; Watson, M. D., Conjugated Polymers from Naphthalene bisimide. *Org. Lett* **2008,** *10*, 5333-5336.

(41) Wang, S.; Sun, H.; Ail, U.; Vagin, M.; Persson, P. O. Å.; Andreasen, J. W.; Thiel, W.; Berggren, M.; Crispin, X.; Fazzi, D.; Fabiano, S., Thermoelectric Properties of Solution-Processed n-Doped Ladder-Type Conducting Polymers. *Adv. Mater.* **2016,** *28*, 10764-10771.

For Table of Contents